Contribution from the Departament de Quîmica Inorgânica, Universitat de Barcelona, Diagonal 647, 08028-Barcelona, Spain, and Departament de Cristal.lografia i Dipòsits Minerals, Universitat de Barcelona, Martî i Franquês s/n, 08028-Barcelona, Spain

New Nickel(II)-Copper(II) Heterodinuclear Complexes with Hexa- and Pentacoordinated Nickel(II) Ions. Magnetostructural Correlations

Albert Escuer,*[1a] Ramon Vicente,[1a] Joan Ribas,[1a] Ramon Costa,[1a] and Xavier Solans[1b]

Received October 29, 1991

Three new heterodinuclear $Cu^{II}Ni^{II}$ complexes of formula $[Ni(cth)Cu(oxpn)](ClO_4)_2$ (**1**), $[Ni(cth)Cu(OHoxpn)](ClO_4)_2$ (**2**) $[Ni(cth)Cu(Me_2oxpn)](ClO_4)_2$ (**3**) in which the nickel(II) ion is octahedrally coordinated, and four new $Cu^{II}Ni^{II}$ complexes with pentacoordinated nickel(II), $[Ni(Me_3[12]N_3)Cu(oxpn)](ClO_4)_2$ (**4**), $[Ni(Me_3[12]N_3)Cu(Me_2oxpn)](ClO_4)_2$ (**5**), $[Ni(Me_4[12]N_3)Cu(oxpn)](ClO_4)_2$ (**6**), and $[Ni(Me_4[12]N_3)Cu(Me_2oxpn)](ClO_4)_2$ (**7**) have been synthesized and characterized. Cth is *d*,*l*-5,5,7,12,12,14-hexamethyl-1,4,8,11-tetraazacyclotetradecane; $Me_3[12]N_3$ is 2,4,4-trimethyl-1,5,9-triazacyclododec-1-ene, $Me_4[12]N_3$ is its 9-methyl derivative; oxpn, OHoxpn, and Me_2oxpn are *N*,*N'*-bis(3-aminopropyl)oxamido and its 2-hydroxo or 2,2'-dimethyl derivatives. The crystal structures of **1** and **5** have been solved. The complex $C_{24}H_{52}N_8O_2NiCu{\cdot}2ClO_4$ (**1**) crystallizes in the monoclinic system, space group $P2_1/a$, with fw = 805.50, $a = 24.704$ (4) Å, $b = 9.802$ (3) Å, $c = 16.084$ (3) Å, $\beta = 105.44$ (3)°, $V = 3754$ (3) Å^3, $Z = 4$, $R = 0.068$, and $R_w = 0.073$. The nickel atom is placed in a distorted octahedral environment. The complex $C_{24}H_{49}N_7O_2NiCu{\cdot}2ClO_4$ (**5**) crystallizes in the monoclinic system, space group $P2_1$, with fw = 788.50, $a = 13.794$ (4) Å, $b = 27.459$ (7) Å, $c = 9.783$ (3) Å, $\beta = 95.80$ (3)°, $V = 3687$ (3) Å^3, $Z = 4$, $R = 0.059$, and $R_w = 0.059$. The nickel atom is placed in an environment intermediate between a trigonal bipyramid and a square pyramid. The magnetic properties of all these compounds have been investigated. The $\chi_M T$ vs T plots for **1**-**7** exhibit the typical shapes for this kind of heterodinuclear complex. Using the Hamiltonian $H = -JS_{Cu}S_{Ni}$, the average J value obtained when nickel(II) is octahedral was found to be ca. -95 cm^{-1}, and when the nickel(II) is pentacoordinated, it is ca. -120 cm^{-1}. Extended Hückel-MO calculations indicate that the doublet-quartet gap should be greater when nickel(II) is pentacoordinated, in agreement with the experimental J values. The EPR spectra (powdered samples or acetonitrile (ACN) solution) of all the complexes show a very intense signal independent of the temperature at approximately $g = 2.2$ and a broad signal at approximately $g = 4$, which vanishes when the temperature is lowered. This is interpreted as being due to an axial ZFS in the excited quartet state.

Introduction

The field of heteropolymetallic systems with different paramagnetic centers is of current interest in connection with spin exchange and charge transfer between metal ions.[2,3] From the literature it is clear that the number of accurate magnetic data on heteropolymetallic compounds is much lower than that for homopolymetallic systems and that the $Ni^{II}Cu^{II}$ complexes represent one of the most widely studied systems.[4-19] However, in all cases reported, nickel(II) is octahedrally coordinated. No example with pentacoordinated nickel(II) has been described, and only EPR spectra have been studied in dinuclear copper(II) complexes doped with pentacoordinated[20-22] nickel(II). Magnetostructural correlations when copper(II) presents octahedral, square-planar or pentacoordinate geometry have been exhaustively studied,[23,24] but no similar study has been found for nickel(II) ions in heteropolynuclear complexes. Starting from the square planar complex cation $[Ni(cth)]^{2+}$ (cth = *d*,*l*-5,5,7,12,12,14-hexamethyl-1,4,8,11-tetraazacyclotetradecane), it is possible to obtain cis-octahedral nickel(II) complexes[25] while from $[Ni(Me_3[12]N_3)]^{2+}$ ($Me_3[12N_3]$ = 2,4,4-trimethyl-1,5,9-triazacyclo-dodec-1-ene) or its derivatives it is possible to obtain pentacoordinated complexes.[26] Their reaction with [Cu(oxpn)] (oxpn) = *N*,*N'*-bis(3-aminopropyl)oxamido) or its hydroxo or methyl derivatives allow the synthesis of new $Cu^{II}Ni^{II}$ heterodi-

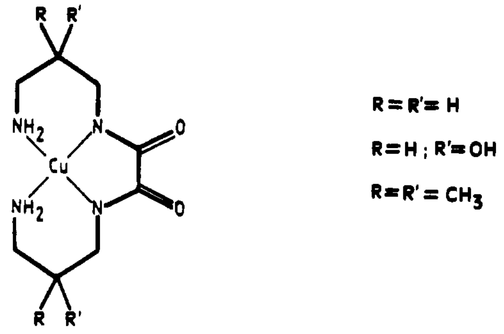

---

[1] (a) Department of Inorganic Chemistry, University of Barcelona. (b) Department of Crystallography, University of Barcelona.

[2] Willet, R. D., Gatteschi, D., Kahn, O., Eds.; *Magneto Structural Correlations in Exchange Coupled Systems*; NATO ASI Series; Reidel: Dordrecht, The Netherlands, 1985.

[3] Kahn, O. *Struct. Bonding* **1987**, *68*, 89.

[4] Bencini, A.; Gatteschi, D. *Mol. Phys.* **1985**, *54*, 969.

[5] Tola, P.; Kahn, O.; Chauvel, C.; Coudanne, H. *Nouv. J. Chim.* **1977**, *1*, 647.

[6] Costes, J. P.; Serra, J. F.; Dahan, F.; Laurent, J. P. *Inorg. Chem.* **1986**, *25*, 2790.

[7] Morgerstern-Badarau, I.; Kahn, O.; Jaud, J.; Galy, J. *Inorg. Chem.* **1982**, *21*, 3050.

[8] Buluggiu, E. *J. Phys. Chem. Solids* **1980**, *41*, 1175.

[9] Bencini, A.; Caneschi, A.; Dei, A.; Gatteschi, D.; Zanchini, C.; Kahn, O. *Inorg. Chem.* **1986**, *25*, 1374.

[10] Lambert, S. L.; Spiro, C. L.; Gagnê, R. R.; Hendrickson, D. N. *Inorg. Chem.* **1982**, *21*, 68.

[11] Luneau, D.; Oshio, H.; Okawa, H.; Koikawa, M.; Kida, S. *Bull. Chem. Soc. Jpn.* **1990**, *63*, 2212.

[12] Journaux, Y.; Kahn, O.; Morgersten-Badarau, I.; Galy, J.; Jaud, J.; Bencini, A.; Gatteschi, D. *J. Am. Chem. Soc.* **1985**, *107*, 6305.

[13] Banci, L.; Bencini, A.; Benelli, C.; Gatteschi, D. *Inorg. Chem.* **1981**, *20*, 1399.

[14] Ojima, H.; Nonoyama, K. *Z. Anorg. Allg. Chem.* **1977**, *429*, 282.

[15] Nakatani, K.; Carriat, J. Y.; Journaux, Y.; Kahn, O.; Lloret, F.; Renard, J. P.; Pei, Y.; Sletten, J.; Verdaguer, M. *J. Am. Chem. Soc.* **1989**, *111*, 5739.

[16] Journaux, Y.; Sletten, J.; Kahn, O. *Inorg. Chem.* **1986**, *25*, 439.

[17] Graziani, R.; Vidali, M.; Rizzardi, G.; Cassellato, H.; Vigato, P. A. *Inorg. Chim. Acta* **1979**, *36*, 145.

[18] Zhang, Z.; Liao, D.; Jiang, Z.; Hao, S.; Yao, X.; Wang, H.; Wang, G. *Inorg. Chim. Acta* **1990**, *173*, 201.

[19] Ribas, J.; Garcîa, A.; Monfort, M. *Polyhedron* **1991**, *10*, 103.

[20] Kokoska, G. F.; Allen, H. C.; Gordon, C. *J. Chem. Phys.* **1967**, *46*, 3020.

[21] Banci, L.; Bencini, A.; Gatteschi, D.; Dei, A. *Inorg. Chim. Acta* **1979**, *36*, L419.

[22] Bencini, A.; Gatteschi, D. *EPR of Exchange Coupled Systems*; Springer-Verlag: Berlin, 1990; p 182.

[23] Kahn, O. *Ang. Chem., Int. Ed. Engl.* **1985**, *24*, 834 and references therein.

[24] Ribas, J.; Garcia, A.; Costa, R.; Monfort, M., Alvarez, S.; Zanchini, C.; Solans, X. *Inorg. Chem.* **1991**, *30*, 841 and references therein.

[25] (a) Pei, Y.; Journaux, Y.; Kahn, O. *Inorg. Chem.* **1988**, *27*, 399. (b) Vicente, R.; Escuer, A.; Ribas, J.; Dei, A.; Solans, X.; Calvet, T. *Polyhedron* **1990**, *9*, 1729.

[26] Martin, J. W. L.; Johnston, J. H.; Curtis, N. F. *J. Chem. Soc., Dalton Trans.* **1978**, 68.

0020-1669/92/1331-2627$03.00/0

Table I. Crystallographic Data for $[Ni(cth)Cu(oxpn)](ClO_4)_2$ (**1**) and for $[Ni(Me_3[12]N_3)Cu(Me_2oxpn)](ClO_4)_2$ (**5**)

	1	**5**
formula	$C_{24}H_{52}Cl_2CuN_8NiO_{10}$	$C_{24}H_{49}Cl_2CuN_7NiO_{10}$
fw	805.50	788.50
temp, K	298	298
space group	$P2_1/a$	$P2_1$
a, Å	24.704 (4)	13.794 (4)
b, Å	9.802 (3)	27.459 (7)
c, Å	16.804 (3)	9.783 (3)
β, deg	105.44 (3)	95.80 (3)
V, Å^3	3754 (3)	3687 (3)
Z	4	4
λ(Mo Kα), Å	0.710 69	0.710 69
d_{cal}, g cm^{-3}	1.411	1.414
μ(Mo Kα), cm^{-1}	12.89	13.10
Abs cor	no	no
$R(F_o)^a$	0.068	0.059
$R_w(F_o)^b$	0.073	0.059

[a] $R(F_o) = \sum||F_o| - |F_c||/\sum|F_o|$. [b] $R_w(F_o) = \sum w||F_o| - |F_c||/\sum w|F_o|$.

nuclear complexes which can facilitate the study of the correlations between magnetic coupling and nickel(II) geometry. In this paper we report the synthesis, characterization, magnetostructural correlations, and theoretical study of seven new $Ni^{II}Cu^{II}$ complexes, with an octahedral (**1**–**3**) or pentacoordinated (**4**–**7**) nickel(II) environment.

Experimental Section

Caution! Perchlorate salts of metal complexes are potentially explosive. Only a small amount of material should be prepared, and it should be handled with caution.

Synthesis of Starting Materials. $[Cu(oxpn)]$,[19,27] $[Cu(Me_2oxpn)]$,[19] $[Cu(OHoxpn)]$,[19] $[Ni(d,l\text{-cth})](ClO_4)_2$,[28] $[Ni_2(OH)_2(Me_3[12]N_3)_2](ClO_4)_2$,[26] and $[Ni_2(OH)_2(Me_4[12]N_3)_2](ClO_4)_2$[29] were prepared as previously described.

Synthesis of the New Heterodinuclear Complexes. The seven new complexes were prepared in a similar way: 1 mmol of the corresponding mononuclear Cu(II) complex was dissolved in 20 mL of water and filtered. To this solution was added 1 mmol of $[Ni(cth)](ClO_4)_2$ dissolved in the minimum amount of water (or 0.5 mmol of $[Ni_2(OH)_2(Me_3[12]N_3)_2](ClO_4)_2$ or $[Ni_2(OH)_2(Me_4[12]N_3)_2](ClO_4)_2$ in aqueous solution (20 mL of neutral solution obtained by neutralization with 10% perchloric acid)) at room temperature with constant stirring. The new compounds immediately precipitated as violet powders in high yields (80–90% approximately). Satisfactory analytical results were obtained for all the complexes. Good crystals of $[Ni(cth)Cu(oxpn)](ClO_4)_2$ (**1**) were obtained by slow evaporation in a methanol/*n*-butanol (1:1) mixture (this complex is insoluble in pure *n*-butanol). Good crystals of $[Ni(Me_3[12]N_3)Cu(Me_2oxpn)](ClO_4)_2$ (**5**) were obtained by slow evaporation of the aqueous mother solution.

Physical Measurements. Infrared spectra (4000–200 cm^{-1}) were recorded from KBr pellets in a Perkin-Elmer 1330 IR spectrophotometer. Electronic spectra were measured in a Shimadzu UV 160 A spectrophotometer, in the 1100–200 nm range. Magnetic measurements were carried out with a Faraday type magnetometer (MANICS DSM8) equipped with an Oxford CF 1200 S helium continuous-flow cryostat working in the temperature range 300–4 K and a Brucker B E15 electromagnet. The magnetic field was 15 000 G approximately. For all compounds the independence of the magnetic susceptibility versus the applied field was checked at room temperature to 1.8 T. Calibration of the instrument was made by a magnetization measurement of a NAJ10 ferrite magnet. Diamagnetic corrections were estimated from Pascal tables. EPR spectra were recorded on powder samples or ACN solutions at X-band frequency with a Bruker ER 200 D spectrometer equipped with a helium continuous flow cryostat. The magnetic field was determined with a Hall probe, and the klystron frequency, with a Hewlett-Packard frequencymeter.

Crystal Data Collection and Refinement. The crystals (0.1 × 0.1 × 0.1 mm) of **1** and (0.1 × 0.1 × 0.2 mm) of **5** were selected and mounted on a Phillips PW-1100 four-circle diffractometer. The crystallographic data, conditions retained for the intensity data collection, and some features of the structure refinement are listed in Table I. Accurate unit cell parameters were determined from automatic centering of 15 reflections ($4 \le \theta \le 12°$) and refined by the least-squares method. Intensities were collected with graphite-monochromatized Mo Kα radiation, using the ω-scan technique, with scan width 0.8° and scan speed 0.03° s^{-1}.

For **1**, 5324 reflections were measured in the range $2 \le \theta \le 25°$ ($\pm h,+k,+l$) range. R_{int} of F^2 was 0.042. A total of 2020 reflections were assumed as observed by applying the conduction $I \ge 2.5\sigma(I)$. For **5**, 4375 reflections were measured in the range $2 \le \theta \le 25°$, 1737 of which were assumed as observed by applying the same condition. In both cases three reflections were measured every 2 h as orientation and intensity control; significant intensity decay was not observed. Corrections were made for Lorentz–polarization but not for absorption. The structure of **1** was solved by the MULTAN method[30] and that of **5** by Patterson synthesis using the SHELXS computer program.[31] The two structures were refined by a full-matrix least-squares method, using the SHELX76 computer program.[32] The function minimized was $\sum w||F_o| - |F_c||^2$, where $w = (\sigma^2|F_o| + 0.061|F_o|^2)^{-1}$, f, f', and f'' were taken from ref 33. For **1** a C_3H_6NO moiety and six O atoms of the ClO_4 ion were located in double positions. A second crystal, obtained in an independent crystallization process, was selected and mounted on a diffractometer, in order to determine a possible "nondisorder" structure. The same result was obtained. A disorder with an occupancy factor of 0.5 was assumed according to height of peaks of Fourier synthesis. A total of 32 H atoms were computed and refined with an overall isotropic temperature factor, using a riding model, while the remaining atoms were refined anisotropically. The final R factor was 0.068 (R_w = 0.073). Number of parameters refined = 424. Maximum shift/esd = 0.3 in z of O(4); Maximum and minimum peaks in final difference synthesis were 0.3 and −0.3 e Å^{-3}, respectively. For **5**, a methylic C atom of a 2-dimethyl-1,3-propanediamine ligand and oxygen atoms of perchlorate ions were located in disorder positions; an occupancy factor of 0.5 was assigned according to maxima of peaks observed in the difference syntheses. The poor quality of the measured intensity did not allow for the location of the hydrogen atoms. The final R factor was 0.059 (R_w = 0.059) for all observed reflections. The number of parameters refined was 470. Maximum shift/esd = 0.1. Maximum and minimum peaks in final difference syntheses were 0.4 and −0.4 e Å^{-3}, respectively. Final atomic coordinates for **1** and **5** are given in Tables II and III, respectively.

Results and Discussion

Description of the Structures: $[Ni(cth)Cu(oxpn)](ClO_4)_2$ (1). The unit cell contains four dinuclear [NiCu] dications and two symmetrically independent sets of four perchlorate anions. Selected bond lengths and angles are listed in Table IV. Other distances and angles may be found in the supplementary material. A view of the dinuclear unit with the atom-labeling scheme and the unit cell are presented in Figure 1.

The nickel atom occupies an asymmetrical octahedral environment consisting of two oxamato oxygen atoms (O(15), O(28)) and two nitrogen atoms (N(5), N(12)) in equatorial positions, and two other nitrogen atoms (N(1), N(8)) in apical positions. As can be seen in Table IV three of these distances are slightly longer than the other three.

The N_4 environment of the copper atom is slightly distorted from square planar to tetrahedral. The distortion evaluated through the distortion parameter introduced by Galy et al.[34] was found to be 2.5%. The N(17), N(21), and N(22) atoms are coplanar, N(26) being 0.23 Å out of plane. The resulting Cu atom-to-mean-plane distance is about 0.03 Å. Intramolecular separation between metal ions is Cu···Ni = 5.32 Å. Perchlorate anions are placed between the *d,l*-cth groups, excluding interactions between the dimeric units.

The crystallographic disorder in the C_3H_6NO moiety and ClO_4^- anions is not significant for the purposes of this study, centered

---

(27) (a) Journaux, Y.; Sletten, J.; Kahn, O. *Inorg. Chem.* **1985**, *24*, 4063. (b) Ojima, H.; Nonoyama, K. *Z. Anorg. Allg. Chem.* **1972**, *389*, 75.

(28) Tait, A. M.; Busch, D. H. *Inorg. Synth.* **1976**, *18*, 4.

(29) Escuer, A.; Vicente, R.; Ribas, J. *Polyhedron* **1992**, *11*, 453.

(30) Main, F.; Fiske, S. E.; Hull, S. L.; Lessinger, L.; Germain, G.; Leclerc, J. P.; Woolfson, M. M. MULTAN. An automatic system of computer programs for crystal structure determination from X-ray diffraction data. University of York, England and University of Louvain, Belgium, 1984.

(31) Sheldrick, G. M. *Acta Crystallogr.* **1990**, *A46*, 467.

(32) Sheldrick, G. M. SHELX. A computer program for Crystal structure determination. University of Cambridge, England, 1976.

(33) *International Tables for X-ray Crystallography*; Kynoch Press: Birmingham, England, 1974.

(34) Galy, J.; Bonnet, J. J.; Anderson, S. *Acta Chem. Scand., Ser. A* **1979**, *A33*, 383.

Table II. Final Atomic Coordinates (×10^4) and Equivalent Isotropic Thermal Parameters (Å^2) and Their Estimated Standard Deviations for [Ni(cth)Cu(oxpn)](ClO$_4$)$_2$ (**1**)

	x/a	y/b	z/c	B_{EQ}[a]
Cu	4968 (1)	5676 (2)	1847 (1)	4.90 (9)
Ni	3174 (1)	7474 (2)	2763 (1)	3.54 (7)
N(1)	2683 (5)	7286 (11)	1443 (7)	5.03 (59)
C(2)	2314 (6)	6148 (16)	1091 (12)	6.02 (87)
C(21)	2711 (9)	4991 (19)	1018 (15)	9.37 (129)
C(22)	1940 (7)	6342 (22)	237 (11)	8.63 (115)
C(3)	1979 (5)	5777 (15)	1740 (9)	4.98 (75)
C(4)	2294 (6)	5274 (14)	2655 (10)	5.10 (82)
C(41)	1855 (7)	4495 (18)	3005 (14)	8.44 (111)
N(5)	2570 (4)	6412 (12)	3194 (7)	4.35 (57)
C(6)	2840 (7)	6021 (20)	4078 (11)	6.95 (102)
C(7)	3175 (7)	7171 (21)	4542 (9)	7.08 (99)
N(8)	3586 (5)	7713 (14)	4120 (7)	5.64 (66)
C(9)	3858 (6)	9045 (19)	4482 (10)	5.90 (89)
C(91)	4398 (7)	9229 (22)	4145 (13)	8.83 (125)
C(92)	4072 (9)	9096 (26)	5435 (12)	11.39 (155)
C(10)	3459 (7)	10156 (20)	4211 (11)	7.00 (102)
C(11)	3249 (6)	10535 (13)	3222 (12)	5.73 (86)
C(111)	2968 (8)	12001 (19)	3108 (16)	10.39 (140)
N(12)	2855 (4)	9505 (9)	2701 (7)	3.85 (52)
C(13)	2674 (7)	9765 (15)	1776 (11)	5.68 (86)
C(14)	2359 (7)	8633 (18)	1299 (10)	6.19 (89)
O(15)	3810 (3)	8200 (8)	2261 (5)	3.67 (39)
C(16)	4153 (5)	7264 (12)	2212 (7)	3.31 (57)
N(17)	4616 (4)	7390 (10)	1933 (6)	4.05 (49)
C(18)	4714 (5)	8777 (14)	1669 (11)	5.64 (77)
C(19)	5334 (6)	8891 (15)	1533 (13)	7.09 (96)
C(20)	5435 (5)	7835 (16)	902 (9)	5.64 (82)
N(21)	5536 (5)	6451 (13)	1289 (8)	5.76 (64)
N(22)	5364 (14)	3987 (23)	1902 (26)	7.39 (184)
C(23)	5276 (16)	3191 (119)	2398 (45)	18.02 (480)
C(24)	4746 (21)	2592 (47)	2589 (36)	7.84 (285)
C(25)	4277 (14)	3472 (46)	2742 (31)	6.02 (226)
N(26)	4370 (13)	4702 (27)	2444 (25)	4.42 (154)
N(22)′	5337 (35)	3374 (82)	1819 (48)	23.78 (683)
C(23)′	5197 (38)	2456 (42)	2216 (58)	16.21 (595)
C(25)′	4278 (25)	3572 (52)	2387 (32)	7.89 (336)
C(24)′	4505 (27)	2526 (58)	1942 (40)	12.98 (398)
N(26)′	4402 (14)	5102 (28)	2239 (20)	3.08 (134)
C(27)	4069 (7)	5878 (14)	2501 (9)	5.25 (82)
O(28)	3634 (3)	5707 (8)	2802 (6)	4.97 (46)
Cl(1)	1192 (2)	11775 (5)	476 (3)	6.48 (23)
Cl(2)	1457 (2)	8929 (5)	3673 (3)	7.81 (26)
O(1)	1451 (14)	12067 (35)	−178 (23)	10.46 (37)
O(1)′	1640 (11)	12017 (25)	117 (17)	6.19 (22)
O(2)	927 (34)	13180 (95)	651 (56)	24.65 (94)
O(2)′	906 (10)	12956 (24)	620 (14)	4.54 (16)
O(3)	1465 (13)	11466 (33)	1306 (21)	8.30 (29)
O(3)′	3572 (12)	5863 (30)	−1211 (19)	8.02 (25)
O(4)	893 (16)	10742 (37)	54 (23)	9.34 (35)
O(4)′	694 (13)	10975 (33)	−3 (19)	8.35 (29)
O(5)	1567 (9)	8609 (23)	2843 (14)	6.34 (17)
O(5)′	1424 (14)	8131 (37)	2966 (22)	3.45 (25)
O(6)	1008 (14)	−478 (34)	3675 (22)	12.46 (29)
O(7)	1147 (32)	−2450 (96)	3796 (54)	16.44 (83)
O(7)′	2038 (19)	9579 (45)	4037 (30)	7.70 (36)
O(8)	1722 (10)	−1588 (26)	4441 (17)	8.97 (20)

[a] $B_{EQ} = 8\pi^2/_3 \sum_i\sum_j U_{ij}\mathbf{A}^*_i\mathbf{A}^*_j\mathbf{A}_i\mathbf{A}_j$.

Table III. Final Atomic Coordinates (×10^4) and Equivalent Isotropic Thermal Parameters (Å^2) and Their Estimated Standard Deviations for [Ni(Me$_3$[12]N$_3$)Cu(Me$_2$oxpn)](CiO$_4$)$_2$ (**5**)

	x/a	y/b	z/c	B_{EQ}[a]
Cu	2403 (3)	5244 (1)	3944 (3)	5.4 (2)
Ni	3093 (3)	3577 (1)	1510 (3)	5.4 (2)
N(1)	2648 (19)	5534 (7)	5912 (23)	6 (1)
C(2)	2936 (24)	5163 (12)	7091 (31)	7 (2)
C(3)	3633 (27)	4813 (12)	6953 (32)	7 (2)
C(31)	3921 (24)	4519 (11)	8286 (28)	6 (2)
C(32)	4586 (27)	5061 (11)	6656 (34)	7 (2)
C(4)	3394 (22)	4402 (9)	5865 (27)	5 (2)
N(5)	2986 (15)	4616 (7)	4474 (24)	4 (1)
C(6)	3021 (20)	4322 (10)	3457 (27)	4 (2)
O(7)	3330 (12)	3883 (6)	3340 (17)	4 (1)
O(8)	2510 (13)	4252 (6)	1067 (19)	5 (1)
C(9)	2599 (22)	4550 (11)	2106 (32)	5 (2)
N(10)	2310 (18)	4975 (9)	2083 (23)	5 (1)
C(11)	1836 (24)	5169 (11)	892 (32)	6 (2)
C(12)	1559 (21)	5698 (9)	828 (32)	4 (2)
C(121)	1253 (24)	5885 (11)	−594 (31)	8 (2)
C(122)	557 (47)	5584 (21)	1515 (60)	6 (4)
C(122)	2699 (39)	5867 (18)	822 (50)	5 (3)
C(13)	1613 (99)	6021 (12)	2090 (46)	9 (3)
N(14)	1913 (18)	5900 (7)	3403 (25)	5 (1)
N(15)	4184 (16)	3086 (7)	2035 (21)	4 (1)
C(16)	4953 (21)	3157 (10)	952 (30)	5 (2)
C(161)	5843 (19)	2865 (10)	1494 (28)	5 (2)
C(162)	5142 (20)	3706 (9)	957 (29)	5 (2)
C(17)	4464 (19)	2907 (9)	−406 (24)	4 (1)
C(18)	3496 (23)	3084 (10)	−1075 (23)	4 (2)
C(181)	3329 (20)	2872 (10)	−2485 (28)	5 (2)
N(19)	2899 (17)	3338 (7)	−475 (20)	3 (1)
C(20)	1896 (23)	3439 (10)	−1095 (28)	5 (2)
C(21)	1107 (20)	3128 (11)	−527 (28)	5 (2)
C(22)	984 (18)	3288 (10)	936 (32)	5 (2)
N(23)	1866 (16)	3214 (7)	1984 (23)	5 (1)
C(24)	2051 (22)	2704 (10)	2413 (28)	5 (2)
C(25)	2966 (23)	2591 (9)	3286 (28)	5 (2)
C(26)	3838 (21)	2583 (9)	2361 (27)	5 (2)
Cl(1)	4159 (4)	6572 (2)	4404 (6)	4.9 (3)
Cl(2)	5201 (6)	1335 (2)	9702 (8)	6.3 (4)
O(11)	6816 (11)	3287 (4)	5456 (13)	7 (1)
O(12)	5194 (26)	3042 (14)	5526 (25)	5 (2)
O(12)′	5239 (26)	3048 (11)	4778 (24)	4 (1)
O(13)	5752 (35)	3652 (16)	4241 (45)	8 (3)
O(13)′	562 (33)	1188 (14)	−136 (44)	6 (2)
O(14)	761 (10)	1466 (5)	1827 (15)	8 (1)
O(21)	−328 (23)	3416 (12)	3706 (30)	9 (2)
O(21)′	−126 (20)	3442 (11)	5926 (29)	6 (2)
O(22)	5718 (25)	912 (10)	−1194 (29)	8 (2)
O(22)′	4630 (21)	968 (10)	−556 (26)	7 (2)
O(23)	1246 (23)	3356 (11)	4884 (31)	8 (2)
O(23)′	6088 (25)	1218 (13)	−216 (34)	6 (2)
O(24)	5725 (21)	869 (11)	840 (33)	7 (2)
O(24)′	5384 (26)	1230 (17)	691 (47)	9 (3)

[a] $B_{EQ} = 8\pi^2/_3 \sum_i\sum_j U_{ij}\mathbf{A}^*_i\mathbf{A}^*_j\mathbf{A}_i\mathbf{A}_j$.

on the arrangement of the magnetic orbitals of the cations and the possible interactions of the dinuclear units in the cell (see magnetic and EPR discussion).

[Ni(Me$_3$[12]N$_3$)Cu(Me$_2$oxpn)](ClO$_4$)$_2$ (5). The unit cell contains four dinuclear [NiCu] dications and two symmetrically independent sets of four perchlorate anions. Selected bond lengths and angles are listed in Table V. Other distances and angles will be found in the supplementary material. A view of the dinuclear unit with the atom-labeling scheme and the unit cell is presented in Figure 2.

The nickel atom occupies an environment intermediate between square pyramidal and trigonal bipyramidal. We have quantified the distortion of the coordination polyhedron around the nickel(II) cation, using the Muetterties and Guggenberger[35] description, and by considering the regular square pyramid (SP) and the ideal trigonal bipyramid (TBP) as the limiting geometries. From the observed dihedral angles, the parameter (0 for tbp and 1 for sp) is found to be 0.51. Consequently, if we consider the nickel(II) environment as tbp, N(19) and O(7) occupy the axial positions and O(8), N(23), and N(15) the equatorial ones; if we consider the environment as sp, then N(23) occupies the axial position and O(8), O(7), N(15), and N(19) occupy the plane positions. The three Ni–N and Ni–O distances are almost equivalent (average value 2.05 Å) (Table V), and Ni–O(7) distance being slightly shorter (1.97 (2) Å). The N(19)–Ni–O(7) angle is 173.2°, near the 180° characteristic for either tbp or sp geometries. All the remaining angles (Table V) are intermediate between those

---

(35) (a) Muertterties, E. L.; Guggenberger, L. J. *J. Am. Chem. Soc.* **1974**, *96*, 1748. (b) Mesa, J. L.; Arriortua, M. I.; Lezama, L.; Pizarro, J. L.; Rojo, T.; Beltran, D. *Polyhedron* **1988**, *7*, 1383. (c) Arriortua, M. I.; Mesa, J. L.; Rojo, T.; Debaerdemaker, T.; Beltran, D.; Stratemeier, H.; Reinen, D. *Inorg. Chem.* **1988**, *27*, 2976.

Table IV. Selected Bond Lengths (Å) and Angles (deg) for $[Ni(cth)Cu(oxpn)](ClO_4)_2$ (**1**)

N(17)–Cu	1.91 (1)	N(12)–Ni	2.134 (9)
N(21)–Cu	2.00 (1)	O(15)–Ni	2.074 (9)
N(22)–Cu	1.91 (3)	O(28)–Ni	2.063 (8)
N(26)–Cu	2.18 (4)	C(16)–O(15)	1.26 (1)
N(22)′–Cu	2.44 (8)	N(17)–C(16)	1.34 (2)
N(26)′–Cu	1.77 (4)	C(27)–C(16)	1.47 (2)
N(1)–Ni	2.15 (1)	C(27)–N(26)	1.39 (3)
N(5)–Ni	2.08 (1)	C(27)–N(26)′	1.27 (4)
N(8)–Ni	2.16 (1)	O(28)–C(27)	1.30 (2)
N(21)–Cu–N(17)	94.9 (5)	N(8)–Ni–N(1)	174.0 (5)
N(22)–Cu–N(17)	173 (1)	N(8)–Ni–N(5)	84.5 (4)
N(22)–Cu–N(17)	86 (1)	N(12)–Ni–N(1)	86.0 (4)
N(26)–Cu–N(17)	88.7 (8)	N(12)–Ni–N(5)	101.1 (5)
N(26)–Cu–N(21)	176.4 (8)	N(12)–Ni–N(8)	90.8 (5)
N(26)–Cu–N(22)	90 (1)	O(15)–Ni–N(1)	86.1 (4)
N(22)′–Cu–N(17)	173 (2)	O(15)–Ni–N(5)	170.0 (4)
N(22)′–Cu–N(21)	92 (2)	O(15)–Ni–N(8)	98.9 (4)
N(26)′–Cu–N(17)	80 (1)	O(15)–Ni–N(12)	88.3 (4)
N(26)′–Cu–N(21)	173 (1)	O(28)–Ni–N(1)	96.8 (4)
N(26)′–Cu–N(22)′	93 (2)	O(28)–Ni–N(5)	90.5 (4)
N(5)–Ni–N(1)	91.1 (4)	O(28)–Ni–N(8)	87.3 (4)

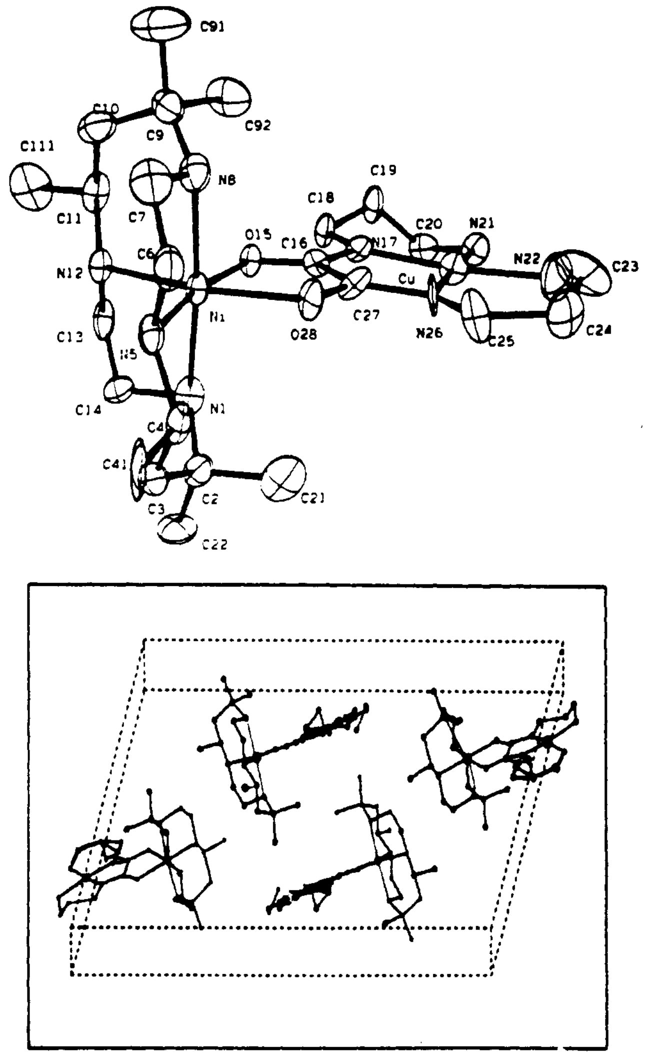

Figure 1. Molecular structure and crystal packing (without the perchlorate anions) for **1**, showing the atom-labeling scheme.

Table V. Selected Bond Lengths (Å) and Angles (deg) for $[Ni(Me_3[12]N_3)Cu(Me_2oxpn)](ClO_4)_2$ (**5**)

O(7)–Ni	1.97 (2)	N(10)–Cu	1.96 (2)
O(8)–Ni	2.05 (2)	N(14)–Cu	1.98 (2)
N(15)–Ni	2.05 (2)	C(9)–C(6)	1.52 (4)
N(19)–Ni	2.04 (2)	C(9)–O(8)	1.30 (3)
N(23)–Ni	2.06 (2)	N(10)–C(9)	1.23 (4)
N(1)–Cu	2.08 (2)	C(6)–N(5)	1.29 (3)
N(5)–Cu	1.95 (2)	O(7)–C(6)	1.29 (3)
O(8)–Ni–O(7)	80.3 (7)	N(10)–Cu–N(5)	84.3 (10)
N(15)–Ni–O(7)	90.1 (7)	N(14)–Cu–N(1)	85.3 (9)
N(15)–Ni–O(8)	155.7 (8)	N(14)–Cu–N(5)	175.7 (10)
N(19)–Ni–O(7)	173.2 (8)	N(14)–Cu–N(10)	96.1 (10)
N(19)–Ni–O(8)	94.6 (8)	C(6)–O(7)–Ni	116.9 (15)
N(19)–Ni–N(15)	92.8 (8)	C(9)–O(8)–Ni	113.6 (17)
N(23)–Ni–O(7)	93.8 (8)	C(9)–N(10)–Cu	110.5 (20)
N(23)–Ni–O(8)	99.9 (8)	C(6)–N(5)–Cu	113.4 (18)
N(23)–Ni–N(15)	103.0 (8)	N(10)–C(9)–C(6)	119.9 (27)
N(23)–Ni–N(19)	91.5 (9)	C(9)–C(6)–N(5)	111.8 (23)
N(5)–Cu–N(1)	93.9 (9)	C(9)–C(6)–O(7)	114.1 (23)
N(10)–Cu–N(1)	174.4 (10)	O(8)–C(9)–C(6)	114.7 (24)

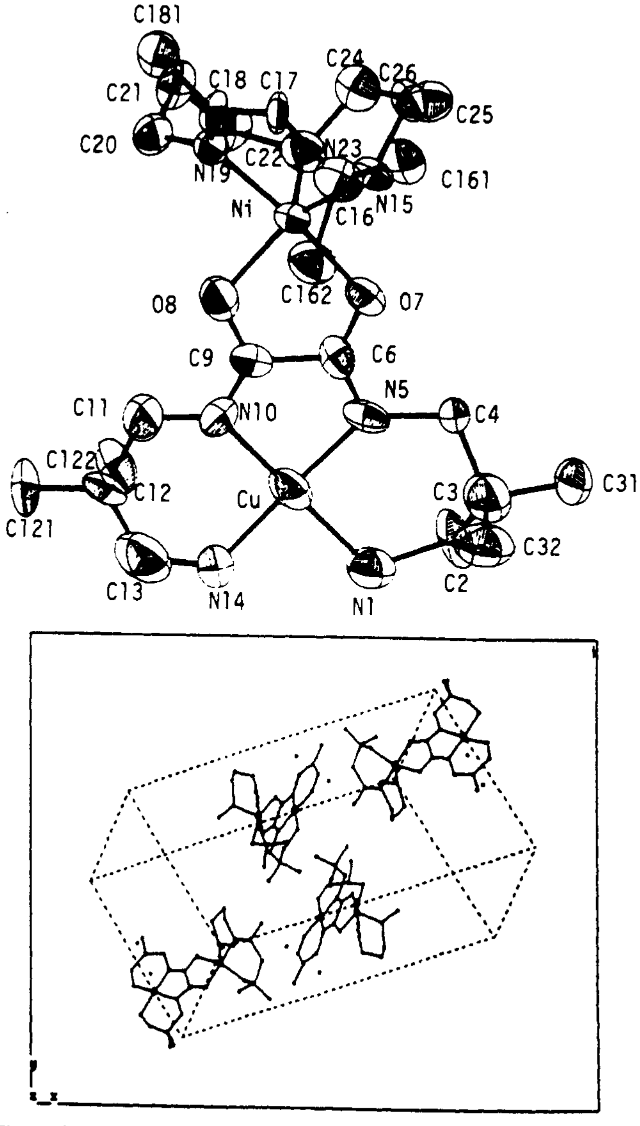

Figure 2. Molecular structure and crystal packing (without the perchlorate anions) for **5**, showing the atom-labeling scheme.

corresponding to tbp or sp geometries. One of the perchlorate anions is placed between the macrocyclic ligands of neighboring molecules. The second is placed between Ni and Cu atoms of each pair of [CuNi] units. The minimum distance Cu···$OClO_3$ or Ni···$OClO_3$ is 4.23 Å.

In compound **5** the N_4 square planar environment of the copper atom is less distorted to tetrahedral than in compound **1**. The distortion evaluated through the distortion parameter introduced by Galy et al.[34] was found to be 1.1%. The resulting copper atom-to-mean-plane distance is about 0.03 Å. The intramolecular separation between metal ions is Cu···Ni = 5.29 Å.

It is important to point out that the slight distortion of the two copper(II) ions (2.2% and 1.1% respectively) may be considered nonsignificant, and consequently, the differences in the magnetic

Table VI. Electronic Spectral Data (ACN Solution) in the Range 1000–400 nm

compd	λ, nm		
1	976	790[a]	553
2	973	791[a]	555
3	943	790[a]	550
4		830[a]	571
5		830[a]	573
6		835[a]	586
7		834[a]	588

[a] Weak.

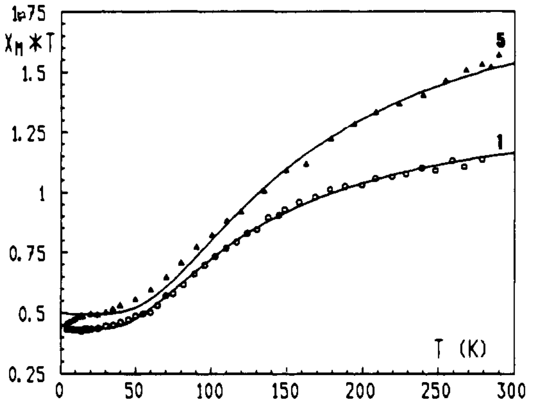

Figure 3. Experimental and calculated (—) temperature dependence of $\chi_M T$ for the dinuclear hexacoordinate nickel(II) complex **1** and the pentacoordinate Ni(II) complex **5**. $\chi_M T$ plots for the other complexes are very similar.

behavior (see below) would only be attributed to the hexa- or pentacoordination of nickel(II).

IR and Electronic Spectra. The IR spectra of all the dinuclear complexes are very similar: the bands attributable to cth, Me_3-[12]N_3, and Me_4[12]N_3 ligands and two strong characteristic bands attributable to the ClO_4^- anion appear at normal frequencies.[36,37] Bands attributable to the central bridging oxamidato ligands, appear at 1600–1630 cm^{-1} (vs, broad).[37] The electronic spectra of the new complexes are very similar and the numerical results are gathered in Table VI. They exhibit three bands: (i) an intense one centered at ca. 550 nm which is interpreted as the envelop of two spin-allowed transitions, the $^3A_2(Ni) \rightarrow {}^3T_1(Ni)$ and the $^2B_2(Cu) \rightarrow {}^2B_1(Cu)$ using the O_h and D_{2h} site symmetries for Ni(II) and Cu(II), respectively; (ii) a weak and narrow band at ca. 790 nm which is assigned to the spin-forbidden transition $^3A_2(Ni) \rightarrow {}^1E(Ni)$ activated by exchange mechanism;[38] (iii) a weak, broad band in the near-infrared region at 950–980 nm which corresponds to the $^3A_2(Ni) \rightarrow {}^3T_2(Ni)$ transition. The third spin-allowed transition for the nickel(II) chromophore $^3A_2(Ni) \rightarrow {}^3T_2(Ni)$, expected in the near-UV region, is hidden by a charge-transfer band due to the copper(II) chromophore.

Magnetic Properties. The $\chi_M T$ vs T plots for complexes **1** and **5** are shown in Figure 3. The $\chi_M T$ values decrease continuously upon cooling and finally reach a plateau below ca. 20 K with $\chi_M T$ = 0.50 cm^3 K mol^{-1} in all cases. This behavior is typical of an antiferromagnetically coupled $Ni^{II}Cu^{II}$ pair with a doublet ground state and a quartet excited state located at an energy $-3J/2$ above.[3] The plateau corresponds to the low-temperature range within which only the doublet ground state is thermally populated. Applying the Hamiltonian $H = -JS_{Cu}S_{Ni}$ the theoretical expression for $\chi_M T$ for such a compound is

$$\chi_M T = (N\beta^2/4k) \left[g_{1/2}^2 + 10 g_{3/2}^2 \exp(3J/2kT)\right] \Big/ \left[1 + 2\exp(3J/2kT)\right]$$

Table VII. Magnetic Parameters (J in cm^{-1}) for Compounds **1**–**7**[a]

compd	J	g(Cu)	g(Ni)
1	−96.3	2.15	2.01
2	−97.6	2.22	2.13
3	−92.8	2.20	2.22
4	−123.1	2.32	2.43
5	−117.8	2.30	2.42
6	−113.7	2.19	2.14
7	−118.5	2.55	2.14

[a] These values were obtained by minimizing the function $R = \sum(\chi T^{calcd} - \chi T^{obs})^2/\sum(\chi T^{obs})^2$. In all cases R was less than 10^{-4}.

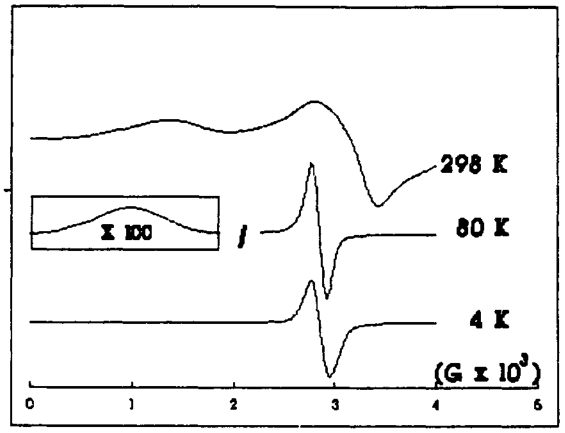

Figure 4. EPR spectra of the dinuclear complex **1** at different temperatures. The other spectra are very similar (see Table VIII).

where $g_{1/2}$ and $g_{3/2}$ are the g factors associated with the doublet and the quartet states, respectively. They are related to the local g factors g_{Ni} and g_{Cu}, assumed to be isotropic through[22,38,39]

$$g_{1/2} = (4g_{Ni} - g_{Cu})/3$$

$$g_{3/2} = (2g_{Ni} + g_{Cu})/3$$

Least-squares fitting of the magnetic data leads to the parameters given in Table VII.

The magnitude order of these parameters (J ca. −100 cm^{-1}) indicates that the doublet-quartet gap ($3J/2$) is ca. 150 cm^{-1}. This shows that the overlap between the magnetic orbitals should be very efficient. In all cases, the J value found when the nickel(II) moiety is pentacoordinated is greater than that found when the same nickel(II) moiety is octahedrally coordinated. The theoretical explanation of this finding from molecular orbital calculations is given below. The slight decrease in the $\chi_M T$ plot for pentacoordinate [CuNi] in the range 10–4 K (Figure 3) can be attributable to low antiferromagnetic interactions between dimeric units through hydrogen bonds of the methyl groups and perchlorates placed between [CuNi] units. In the expression of the magnetic susceptibility, the local distortion from O_h symmetry has not been considered. This should not affect the values of the exchange constants, but it could also explain the decay of $\chi_M T$ below 10 K, for pentacoordinated [CuNi].

EPR. The g values of powdered or ACN solutions of the new heterodinuclear complexes at several temperatures are shown in Table VIII. The seven dinuclear complexes present very similar behavior. In Figure 4, as a typical example, the spectrum of **1** is shown. At room temperature the powdered samples exhibit a very large intense band centered at g = 2.13–2.20 and a large band centered at g = 4.70–4.85. The intensity of the first band (g ca. 2.2) is independent of temperature; instead the low-field band vanishes when the temperature falls and disappears at liquid He temperature. In frozen ACN solutions, the behavior is similar, the two bands (g ca. 2.2 and $g > 4$) being narrower and sharper. This behavior does not correspond to that of a simple ground

---

(36) Curtis, N. F. *J. Chem. Soc., Dalton Trans.* **1964**, 2644.

(37) Nakamoto, K. *Infrared and Raman Spectra of Inorganic and Coordination Compounds*, 4th ed.; J. Wiley: New York, 1986.

(38) Gatteschi, D.; Bencini, A. EPR spectra of oligonuclear complexes. In ref 2, p 241.

(39) Journaux, Y.; Sletten, J.; Kahn, O. *Inorg. Chem.* **1986**, *25*, 439.

doublet state. Assuming, from spectroscopic data, that the two sets of complexes are very similar, knowledge of the structure of one of the hexa- and pentacoordinated complexes would allow us to assume that the low-field *g* factors cannot be attributed to a dimerization of dinuclear entities, as has been reported by Journaux et al.[16] in other [CuNi] complexes. Gatteschi et al.,[13] have indicated that if the *g* values in CuNi pairs correspond to a $S = {}^3/_2$ state largely split in a zero magnetic field, at least one *g* value should be larger than 4, if the true *g* values of the pair are close to 2. This is the explanation that we assume for our seven complexes: the presence of a moderately strong splitting at zero field of the excited quartet state, which gives rise to two Kramer's doublets $|{}^3/_2, \pm{}^1/_2\rangle$ and $|{}^3/_2, \pm{}^3/_2\rangle$. Assuming an axial symmetry in the ZFS, the allowed $|{}^3/_2, -{}^1/_2\rangle \rightarrow |{}^3/_2, {}^1/_2\rangle$ transition will produce two anisotropic signals: a *g* near the g_e value (ca. 2.2) and a *g* at approximately half-field (*g* ca. 4.5). As the quartet is depopulated when the temperature is lowered, as indicated by susceptibility measurements, both signals disappear, only the isotropic signal remaining (*g* ca. 2.2) which corresponds to the allowed $|{}^1/_2, -{}^1/_2\rangle \rightarrow |{}^1/_2, {}^1/_2\rangle$ transition in the $S = {}^1/_2$ ground state.

Finally, the EPR spectra of pentacoordinated complexes (**4**–**7**), are slightly different from those of hexacoordinated derivatives (**1**–**3**) (Table VIII): the *g* values for (**4**–**7**) are greater (2.25–2.30) than the *g* values for (**1**–**3**) (2.18–2.20). Taking into account that *g* values have a contribution of g_{Cu} and g_{Ni}, these differences are not surprising. Effectively, the geometry around the Ni(II) pentacoordinated ions is intermediate between square pyramid and trigonal bipyramid (see discussion of structures). In the latter case, the spin–orbit coupling can not be completely excluded, and consequently, the *g* values can vary considerably from 2.0.

MO Calculations. Extended Hückel-MO[40] calculations have been performed on the structurally characterized dinuclear complexes with the modified Wolfsberg–Helmholtz formula.[41] The atomic parameters used for copper and nickel were taken from the literature,[42] while those for C, O, N, and H were standard.

In order to center this analysis on the coordination environment of the nickel(II) cations, the geometry of both dinuclear species has been modeled as shown

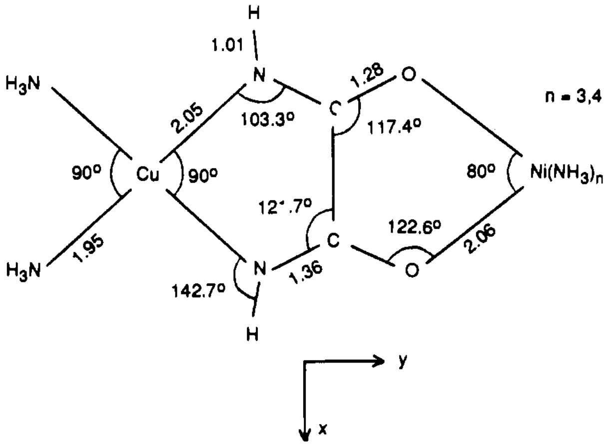

The copper(II) coordination has been idealized as square planar and located in such a way that all the non-hydrogen atoms in the $[(NH_3)_2Cu(C_2O_2N_2H_2)Ni]^{2+}$ portion lie in the *xy* plane. This portion results symmetric with regard to the *yz* plane, and identical in both dinuclear cations. The nickel–ammonia ligand fragments were built up so that bond and dihedral angles would correspond to the original structures, but bond lengths were fixed at 2.06 Å in order to minimize effects other than geometrical.

The MO interaction diagram is summarized in Figure 5. It shows the interactions between the lone pair MO's of the bridging oxamidato ligand and the magnetic orbitals of the metallic atoms. Hexacoordinated nickel(II) cations are shown in the left; pentacoordinate cations are to the right. The magnetic orbital (mainly d_{xy}) of the copper(II) cation and the relevant lone pairs MO's for the oxamidato residue given as n_1 and n_2 are shown in the middle. One such orbital, n_1, has most of its electron density located in the N atoms and hybridized toward the copper atom. In contrast, n_2 is essentially localized at the O atoms and hybridized toward the nickel.

The better energy and symmetry match between n_1 and the d_{xy} orbital of the copper atom leads to stronger interaction. Consequently, the LUMO is formed in the two cases (φ_1 and φ_1') by the same antibonding combination of both orbitals.

When nickel atoms exhibit hexacoordination, their d_{xy} and d_{z^2} magnetic orbitals exhibit dissimilar energies due to the different participation of the ligands. The most antibonding character of the d_{z^2} combination locates it at the upper energy, slightly increased by $3p_z$ hybridization. This forms the SOMO (singly occupied molecular orbital) φ_2, which contains the unpaired electron in the low-energy configuration. Finally, the remaining n_2 and Ni d_{xy} MO's have the appropriate energy and symmetry to form an antibonding combination (φ_3) which is placed in energy not far below the SOMO, in a manner similar to an octahedral e_g energy set.

Table VIII. *g* Values for Compounds **1**–**7** Obtained from EPR Spectra at Variable Temperatures[a]

	298 K	80–100 K		4 K	
compd	powder	powder	ACN soln	powder	ACN soln
1	4.71	4.70 (vw)	4.80 (w)		4.40 (vw)
	2.19	2.20	2.20	2.20	2.20
2	4.85	4.80 (vw)	4.80 (w)		
	2.13	2.15	2.18	2.20	2.18
3	4.85	4.85 (vw)	4.80 (w)		4.38 (vw)
	2.18	2.18	2.20	2.20	2.18
4	4.5 (sh)	4.80 (w)	4.70 (w)	4.72 (vw)	4.44 (vw)
	2.25	2.25	2.25	2.26	2.25
5	5.0 (sh)	4.70 (w)	5.01 (vw)	4.57 (vw)	4.47 (vw)
	2.15	2.25	2.25	2.25	2.25
6			5.30 (w)	4.85 (vw)	4.76 (vw)
	2.37	2.31	2.26	2.28	2.25
7	5.0 (sh)	4.55 (w)	4.80 (w)	4.61 (vw)	4.60 (vw)
	3.28 (w)	2.30	2.31	2.30	2.30
	2.19				

[a] The bands at *g* ca. 2.2 are very strong in all cases. In solid state they are very broad, especially for pentacoordinated nickel(II) complexes (**4**–**7**) (from 0–5000 G). For this reason, the band at low field is overlapped (**6**) or appears only as a shoulder (**4**, **5**, **7**).

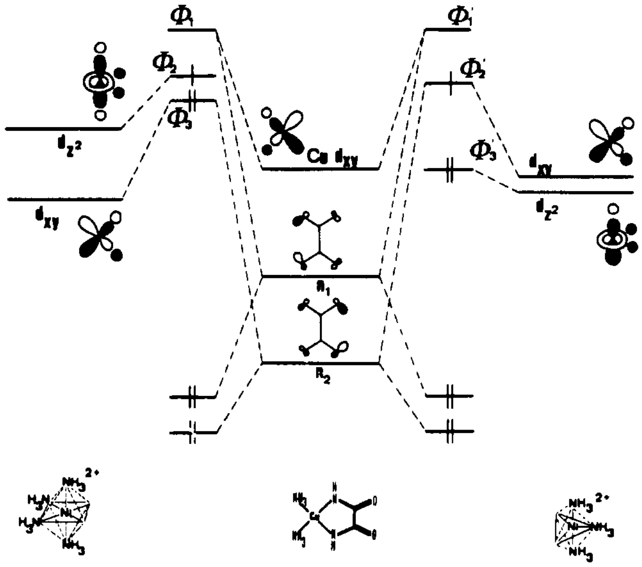

Figure 5. Orbital diagram for the interaction of the unpaired electrons of $Ni^{II}L_4$ (left) and $Ni^{II}L_3$ (right) fragments, with both the $Cu^{II}L_2$ fragments and the lone pairs of the oxamidato bridge.

---

(40) Hoffmann, R. *J. Chem. Phys.* **1963**, *39*, 1397.

(41) Ammeter, J. H.; Burgi, H. B.; Thibeault, J. C.; Hoffmann, R. *J. Am. Chem. Soc.* **1978**, *100*, 3686.

(42) Hay, P. J.; Thibeault, J. C.; Hoffmann, R. *J. Am. Chem. Soc.* **1975**, *97*, 4884.

The pentacoordinate Ni case is presented on the right side of Figure 5. The fact that one of the equatorial ammonia ligands becomes noncoplanar, together with the absence of one axial ligand, makes the two Ni magnetic orbitals closer in energy, with the d_{z^2} combination below the d_{xy} one. This latter combination interacts strongly with the n_2 orbital of the bridging oxamidato, making up the SOMO φ_2'. The d_{z^2} magnetic orbital remains lower and well separated in energy (φ_3') according to the classical pentacoordination scheme.

If we consider the antiferromagnetic part of the doublet–quartet gap, related to the monoelectronic promotion energy of one electron placed in φ_3 (φ_3') to φ_1 (φ_1'), it is easy to realize that the pentacoordinated dinuclear complex should have a stronger antiferromagnetic coupling constant than the hexacoordinate complex.

It is worth noting that, in the absence of correlation and polyelectronic corrections, the electronic doublet constituted mainly by the SOMO, which contains the unpaired electron, has a strong Ni d_{z^2} character (83%) in the hexacoordinate dinuclear Ni complex, while it is Ni d_{xy} (68%) in the pentacoordinate complex.

Acknowledgment. We are very grateful for the financial assistance from the CICYT (Grant No. MAT88-0545). We thank Andrea Dei (Dipartimento di Chimica, Universita di Firenze), for helpful suggestions and stimulating discussions.

Registry No. **1**, 141090-75-7; **2**, 141090-79-1; **3**, 141090-77-9; **4**, 141090-81-5; **5**, 141090-85-9; **6**, 141090-83-7; **7**, 141090-88-2; [Cu(oxpn)], 20102-49-2; [Cu(Me_2oxpn)], 21780-20-1; [Cu(OHoxpn)], 141090-86-0; [Ni(*d*,*l*-cth)]$(ClO_4)_2$, 15392-95-7; $[Ni_2(OH)_2(Me_3[12]N_3)_2](ClO_4)_2$, 66756-81-8; $[Ni_2(OH)_2(Me_4[12]N_3)_2](ClO_4)_2$, 74911-34-5.

Supplementary Material Available: Text giving experimental details of the structure determination for **1** and **5** and tables of complete crystallographic data for **1** and **5**, bond distances and angles for **1** and **5**, anisotropic thermal parameters for **1** and **5**, and hydrogen atom coordinates for **1** (10 pages); tables of calculated and observed structure factors (17 pages). Ordering information is given on any current masthead page.

Contribution from SFA Inc., Landover, Maryland 20785, the Chemistry Division, Code 6120, and Laboratory
for the Structure of Matter, Code 6030, Naval Research Laboratory, Washington, D.C. 20375-5000,
and the Department of Chemistry, Catholic University, Washington, D.C. 20064

Synthesis, Structure, and Magnetic Properties of $Cu_4(\mu\text{-}OCMe_3)_6[OC(CF_3)_3]_2$ and $Cu_3(\mu\text{-}OCMe_3)_4[OC(CF_3)_3]_2$

A. P. Purdy,*[,1] C. F. George, and G. A. Brewer

Received October 10, 1991

The reaction of a moderate excess of perfluoro-*tert*-butyl alcohol (H[PFTB]) with $[Cu(OCMe_3)_2]_n$ in hydrocarbon solvents affords two primary products, $Cu_4(\mu\text{-}OCMe_3)_6[PFTB]_2$ (**1**) and $Cu_3(\mu\text{-}OCMe_3)_4[PFTB]_2$ (**2**), with their relative amounts determined by the reaction stoichiometry. Compound **1** is purified by recrystallization, and **2** is isolated by sublimation of a mixture of **1** and **2**. Both compounds have well-resolved NMR spectra ($\nu_{1/2}$ = 45–90 Hz) and no X-band ESR spectra, indicative of a short electron relaxation time. Compound **1** crystallizes in space group $P\bar{1}$ [fw = 1162.9, a = 10.609 (3) Å, b = 10.667 (3) Å, c = 11.151 (3) Å, α = 100.69 (3)°, β = 95.37 (3)°, γ = 99.65 (3)°, V = 1212.3 (7) Å^3, Z = 1 (two half-molecules), d_{calcd} = 1.593 g/cm^3, $F(000)$ = 588, μ = 18.43 cm^{-1}, T = 295 K]. It consists of three Cu_2O_2 linked twisted rings with bridging $OCMe_3$ groups and two terminal PFTB groups, where the central Cu atoms are 4-coordinate and the two outer Cu atoms are 3-coordinate. The $\{CuO_3\}$ moieties are Y-shaped and planar [terminal Cu–O = 1.797 (5) Å, bridging 3-coordinate Cu–O = 1.856 (4) and 1.865 (4) Å, and bridging 4-coordinate Cu–O = 1.947 Å (average)]. Magnetic measurements (77–300 K) show both **1** and **2** to be antiferromagnetically coupled. The magnetic data for **1** fit a theoretical equation for a linear centrosymmetric tetranuclear d^9 system [J = −131.6 (0.6) cm^{-1}], and the data for **2** fit the corresponding trinuclear equation [J = −114.4 (1.5) cm^{-1}].

Copper(II) alkoxide chemistry has advanced considerably in the last decade, in part due to the discovery of cuprate superconductors and the resulting search for new molecular precursors.[2] As fluorinated alkoxides are often much more volatile than their hydrocarbon counterparts,[3] we sought to prepare fluorinated copper(II) alkoxides by two distinct routes. Metathesis/salt elimination, a standard preparative method for alkoxides, allowed the synthesis of the first crystallographically characterized 3-coordinate Cu(II) complex, $Ba\{Cu[OCMe(CF_3)_2]_3\}_2$, as well as a highly volatile compound which was tentatively identified as $Cu_4[OC(CF_3)_3]_7$.[4] Alcohol-interchange reactions (eqs 1 and 2)

$$M(OR)_x + xR'OH \rightleftharpoons M(OR')_x + xROH \qquad (1)$$

$$M(OR)_x + yR'OH \rightleftharpoons M(OR)_{x-y}(OR')_y + yROH \qquad (2)$$

are another common synthetic method for metal alkoxides[5] and have been used for Cu(II) systems.[2a–c] Replacement of the OR groups by OR′ is often incomplete (eq 2) when bulky alkoxides and/or alcohols are involved or when the starting alkoxide has both strongly bound bridging and more easily replaced terminal alkoxy groups.[2g,5] Also, recent work has shown that approximately 50% substitution of *tert*-butoxy groups occurred in reactions between copper(I) *tert*-butoxide [$(CuOCMe_3)_4$] and various fluorinated alcohols.[6] In our study of alcoholysis reactions between $[Cu(OCMe_3)_2]_n$ and two common fluorinated alcohols, $(F_3C)_3COH$ (H[PFTB]) and $Me(F_3C)_2COH$ (H[HFTB]), partial replacement of the *tert*-butoxide ligands occurred. This paper includes an account of those alcoholysis reactions, a crystallo-

---

(1) SFA Inc. Currently at NRL, Code 6120.

(2) (a) Goel, S. C.; Kramer, K. S.; Gibbons, P. C.; Buhro, W. E. *Inorg. Chem.* **1989**, *28*, 3620–3622. (b) Horowitz, H. S.; McLain, S. J.; Sleight, A. W.; Drulinger, J. D.; Gai, P. L.; Vanhavelaar, M. J.; Wagner, J. L.; Biggs, B. D.; Poon, J. J. *Science* **1989**, *243*, 66–69. (c) Goel, S. C.; Kramer, K. S.; Chaing, M. Y.; Buhro, W. E. *Polyhedron* **1990**, *9*, 611. (d) McMullen, A. K.; Tilley, T. D.; Rheingold, A. L.; Geib, S. J. *Inorg. Chem.* **1989**, *28*, 3772. (e) Sauer, N. N.; Garcia, E.; Salazar, K. V.; Ryan, R. R.; Martin, J. A. *J. Am. Chem. Soc.* **1990**, *112*, 1524. (f) Rupich, M. W.; Lagos, B.; Hackey, J. P. *Appl. Phys. Lett.* **1989**, *55*, 2447–2449. (g) Caulton, K. G.; Hubert-Pfalzgraf, L. G. *Chem. Rev.* **1990**, *90*, 969. (h) Singh, J. V.; Baranwal, B. P.; Mehrotra, R. C. *Z. Anorg. Allg. Chem.* **1981**, *477*, 235–240. (i) Banait, J. S.; Pahil, P. K. *Synth. React. Inorg. Met.-Org. Chem.* **1988**, *18*, 309–315. (j) Purdy, A. P.; George, C. F.; Callahan, J. H. *Inorg. Chem.* **1991**, *30*, 2812–2819.

(3) Willis, C. J. *Coord. Chem. Rev.* **1988**, *88*, 133–202.

(4) Purdy, A. P.; George, C. F. *Inorg. Chem.* **1991**, *30*, 1969–1970.

(5) Bradley, D. C.; Mehrotra, R. C.; Gaur, D. P. *Metal Alkoxides*; Academic Press: London, 1978.

(6) Gross, M. E. *J. Electrochem. Soc.* **1991**, *138*, 2422–2426.

0020-1669/92/1331-2633$03.00/0